A Posteriori Error Estimates in Maximum Norm for Interior Penalty Discontinuous Galerkin Approximation of the Obstacle Problem

B. Ayuso de Dios, T. Gudi, and K. Porwal

1 Introduction

Adaptive finite element method (AFEM) is an effective numerical tool for solving linear and nonlinear PDEs. A proper local refinement plays a key role in AFEM and relies on proper a-posteriori error estimators. In this contribution, we introduce a pointwise a posteriori error estimator for the symmetric interior penalty discontinuous Galerkin (SIPG) approximation of the elliptic obstacle problem. The elliptic obstacle problem is a prototype of the elliptic variational inequalities of the first kind. This problem exhibits the free boundary and appears in various processes in engineering and physical sciences such as elasto-plasticity, dam problem and mathematical finance [3]. A-posteriori error analysis in maximum norm for conforming approximation of obstacle problems is given in the seminal works [6, 7]. For discontinuous Galerkin (DG) approximation, the a-posteriori error analysis in energy norm is contained in [4]. In the maximum norm, to the best of our knowledge, the results in [1] are the first in this direction. Here, due to space limitation, we state the reliability result and focus on its numerical verification and validation. Details on the analysis as well as further discussion can be found in [1].

Blanca Ayuso de Dios
Dipartimento di Matematica e Applicazioni, Università di Milano-Bicocca, Milan, Italy, e-mail: blanca.ayuso@unimib.it

T. Gudi
Department of Mathematics, Indian Institute of Science, Bangalore - 560012, e-mail: gudi@math.iisc.ac.in

K. Porwal
Department of Mathematics, Indian Institute of Technology Delhi - 110016 e-mail: kamana@maths.iitd.ac.in

2 The elliptic obstacle problem

Let $\Omega \subset \mathbb{R}^d,\ d = 2, 3$ be a bounded, polygonal ($d = 2$) or polyhedral ($d = 3$) domain with boundary $\partial\Omega$. Let $f \in L^\infty(\Omega)$ and the obstacle $\chi \in H^1(\Omega) \cap C^0(\overline{\Omega})$ be such that $\chi \leq 0$ on $\partial\Omega$. The variational formulation of the obstacle problem then reads: find $u \in \mathcal{K}$ such that

$$\int_\Omega \nabla u \cdot \nabla(u - v)\, dx \leq (f, u - v) \quad \forall v \in \mathcal{K} := \{v \in H_0^1(\Omega) : v \geq \chi \ \text{ a.e. in } \Omega\}\ , \quad (1)$$

where $(\cdot, \cdot)$ refers to the $L^2(\Omega)$ inner-product and $\mathcal{K}$ is the so-called set of admissible displacements which is a non-empty, closed and convex set. In (1), the solution u could be regarded as the equilibrium position of an elastic membrane subject to the load f whose boundary is held fixed ($u \in H_0^1(\Omega)$) and which is constrained to lie above the given obstacle χ. Such constraint results in non-linearity inherent to the PDE. The contact and non-contact sets of the exact solution u are defined as

$$\mathbb{C} := \{x \in \Omega : u(x) = \chi(x)\}^o, \qquad \mathbb{N} := \{x \in \Omega : u(x) > \chi(x)\}.$$

The continuous Lagrange multiplier $\sigma(u) \in H^{-1}(\Omega)$ is defined by

$$\langle \sigma(u), v\rangle = (f, v) - (\nabla u, \nabla v), \quad \forall v \in H_0^1(\Omega), \quad (2)$$

where $\langle \cdot, \cdot \rangle$ denotes the duality pairing of $H^{-1}(\Omega)$ and $H_0^1(\Omega)$. From (2) and (1), it follows that

$$\langle \sigma(u), v - u\rangle \leq 0, \quad \forall v \in \mathcal{K}.$$

In particular, $\sigma(u) = 0$ on the non-contact set $\mathbb{N}$. The classical theory of Stampacchia [3, Chapter 1, page 4] guarantees the existence and uniqueness of the solution. Notice, however that the solution operator is not only non-linear and non-differentiable, but it is strikingly not one-to-one (observe that any variation in f within the contact set might or might not result in a variation in the solution u).

3 The Symmetric Interior Penalty method

Basic Notations and Finite Element spaces

Let $\mathcal{T}_h$ be a shape-regular family of partitions of Ω into triangles or tetrahedra T and let h_T denote the diameter of each $T \in \mathcal{T}_h$ and set $h_{min} = \min\{h_T : T \in \mathcal{T}_h\}$. We denote by $\mathcal{E}_h^o$ and $\mathcal{E}_h^\partial$ the sets of all interior and boundary edges/faces, respectively, and we set $\mathcal{E}_h = \mathcal{E}_h^o \cup \mathcal{E}_h^\partial$. The *average* and *jump* trace operators are defined in the usual way: let T^+ and T^- be two neighbouring elements, and $\mathbf{n}^+$, $\mathbf{n}^-$ be their outward normal unit vectors, respectively ($\mathbf{n}^\pm = \mathbf{n}_{T^\pm}$) and let $\zeta^\pm$ be the restriction of ζ to $T^\pm$. We set:

$$2\{\zeta\} = (\zeta^+ + \zeta^-), \quad [\![\, \zeta \,]\!] = \zeta^+\mathbf{n}^+ + \zeta^-\mathbf{n}^- \qquad \text{on } w \in \mathcal{E}_h^o,$$

and on $e \in \mathcal{E}_h^\partial$ we set $[\![\, \zeta \,]\!] = \zeta\mathbf{n}$. We will also use the notations

$$(u,w)_{\mathcal{T}_h} = \sum_{T\in\mathcal{T}_h}\int_T uw\,dx, \qquad \langle u,w\rangle_{\mathcal{E}_h} = \sum_{e\in\mathcal{E}_h}\int_e uw\,ds \quad \forall\, u,w \in V.$$

Let $\mathbb{P}^1(T)$ be the space of linear polynomials on T and $\mathcal{V}_T$ denotes the set of vertices of the simplex T. We denote by V_h and V_h^{conf} the discontinuous and conforming finite element spaces defined respectively, by

$$V_h = \left\{ v \in L^2(\Omega) \;:\; v_{|_T} \in \mathbb{P}^1(T)\ \forall T \in \mathcal{T}_h \right\}, \quad V_h^{conf} = V_h \cap H_0^1(\Omega)\,. \tag{3}$$

Let $\chi_h \in V_h^{conf}$ be the nodal Lagrange linear interpolant of χ. We define the discrete analogue of $\mathcal{K}$ by

$$\mathcal{K}_h := \{v_h \in V_h : v_h|_T(p) \geq \chi_h(p),\ \ \forall p \in \mathcal{V}_T,\ \ \forall T \in \mathcal{T}_h\} \neq \emptyset,$$

which is a nonempty, closed and convex subset of V_h. Note that, $\mathcal{K}_h \nsubseteq \mathcal{K}$.
• *SIPG method:* The method reads: find $u_h \in \mathcal{K}_h$ such that

$$\mathcal{A}_h(u_h, u_h - v_h) \leq (f, u_h - v_h) \qquad \forall\, v_h \in \mathcal{K}_h, \tag{4}$$

where the SIPG bilinear form $\mathcal{A}_h(\cdot,\cdot)$ is defined as:

$$\mathcal{A}_h(u,w) = (\nabla u, \nabla w)_{\mathcal{T}_h} - \langle\{\nabla u\}, [\![\, w \,]\!]\rangle_{\mathcal{E}_h} - \langle [\![\, u \,]\!], \{\nabla w\}\rangle_{\mathcal{E}_h} + \langle S_e [\![\, u \,]\!], [\![\, w \,]\!]\rangle_{\mathcal{E}_h}\,, \tag{5}$$

with $S_e = \alpha_e h_e^{-1}$, $\alpha_e \geq \alpha^* > 0$, $\forall\, e \in \mathcal{E}_h$ and h_e the length of the edge/face e. Following [8, 4], we define the discrete Lagrange multiplier $\sigma_h \in V_h$:

$$\langle \sigma_h, v_h\rangle_h := (f, v_h) - \mathcal{A}_h(u_h, v_h) \quad \forall v_h \in V_h, \tag{6}$$

where $\langle\cdot,\cdot\rangle_h$ is given by

$$\langle w_h, v_h\rangle_h := \sum_{T\in\mathcal{T}_h}\int_T \mathcal{I}_h(w_h|_T v_h|_T)\,dx = \sum_{T\in\mathcal{T}_h}\frac{|T|}{d+1}\sum_{p\in\mathcal{V}_T} w_h(p)v_h(p),$$

with $\mathcal{I}_h$ denoting the nodal Lagrange linear interpolation operator. The use of the $\langle\cdot,\cdot\rangle_h$ inner product in the definition (6) of σ_h allows for localizing σ_h at the vertices of the partition, which facilitates the implementation. The discrete contact and non-contact sets relative to u_h, are defined by:

$$\mathbb{C}_h := \{T \in \mathcal{T}_h : u_h(p) = \chi_h(p)\ \forall\, p \in \mathcal{V}_T\}, \quad \mathbb{N}_h := \{T \in \mathcal{T}_h : u_h(p) > \chi_h(p)\ \forall\, p \in \mathcal{V}_T\},$$

and the free boundary set is given by $\mathbb{M}_h = \mathcal{T}_h \setminus (\mathbb{C}_h \cup \mathbb{N}_h)$. Using (6) and the discrete problem (4), we obtain that $\langle \sigma_h, v_h - u_h\rangle_h \leq 0 \quad \forall\, v_h \in \mathcal{K}_h$, from which it can be further deduced that $\sigma_h(p) = 0$ on p vertex of $T \subset \mathbb{N}_h$.

4 Reliable a posteriori error estimates in maximum norm

We now define the error estimators that enter in full error estimator η_h :

$$\eta_1 = \max_{T\in\mathcal{T}_h} \|h_T^2(f-\sigma_h)\|_{L^\infty(T)}, \qquad \eta_2 = \max_{T\in\mathbb{C}_h\cup\mathbb{M}_h} \|h_T^2\nabla\sigma_h\|_{L^d(T)},$$
$$\eta_3 = \max_{e\in\mathcal{E}_h^o} \|h_e[\![\nabla u_h]\!]\|_{L^\infty(e)}, \qquad \eta_4 = \|[\![u_h]\!]\|_{L^\infty(\mathcal{E}_h)},$$
$$\eta_5 = \|(\chi-u_h)^+\|_{L^\infty(\Omega)}, \qquad \eta_6 = \|(u_h-\chi)^+\|_{L^\infty(\{\sigma_h<0\})} .$$

The full a-posteriori error estimator η_h is then defined as:

$$\eta_h = |\log h_{min}|\Big(\eta_1+\eta_2+\eta_3+\eta_4\Big)+\eta_5+\eta_6$$

Theorem 1 *Let $u \in \mathcal{K}$ and $u_h \in \mathcal{K}_h$ be the solution of* (1) *and* (4)*, respectively. Then,*

$$\|u-u_h\|_{L^\infty(\Omega)} \lesssim \eta_h$$

The proof of the theorem is technical and we refer to [1] for the details as well as the results regarding local efficiency of the estimator.

5 Numerical Results

To solve (4), we use the iterative *primal dual active set method* [5]. We briefly describe the algorithm in the present setting.
Primal dual active set method: Let $\lambda_h \in V_h$ be defined by setting for every $T \in \mathcal{T}_h$, $p \in \mathcal{V}_T$ $\lambda_h(p) := \frac{|T|}{d+1}\sigma_h(p)$. Then equation (6) can be rewritten as

$$\mathcal{A}_h(u_h,v_h) + \sum_{T\in\mathcal{T}_h}\sum_{p\in\mathcal{V}_T}\lambda_h(p)v_h(p) = (f,v_h) \quad \forall v_h \in V_h. \tag{7}$$

The so-called complementarity conditions are then given by: $\forall p \in \mathcal{V}_T$, $T \in \mathcal{T}_h$

$$\lambda_h(p) \le 0, \quad u_h(p) \ge \chi_h(p) \quad \text{and} \quad \sum_{T\in\mathcal{T}_h}\sum_{p\in\mathcal{V}_T}\lambda_h(p)(u_h(p)-\chi_h(p)) = 0 . \tag{8}$$

After choosing Lagrangian linear basis for V_h in (3), with $N = \dim(V_h)$, we denote by $\mathbb{A} \in \mathbb{R}^{N\times N}$ and $\boldsymbol{F} \in \mathbb{R}^N$ the matrix and vector representation of $\mathcal{A}_h(\cdot,\cdot)$ in (5) and the right hand side in (4), respectively. Similarly, $\boldsymbol{U}, \boldsymbol{\chi}, \boldsymbol{\Lambda} \in \mathbb{R}^N$ denote respectively the vector representations of u_h, χ_h and λ_h. The algebraic formulation of (7)-(8) reads:

$$\mathbb{A}\,\boldsymbol{U} + \mathbb{I}\,\Lambda = \boldsymbol{F}, \quad (\Lambda, \boldsymbol{U}-\boldsymbol{\chi}) = 0, \quad \Lambda \le 0, \quad \boldsymbol{U} \ge \boldsymbol{\chi}, \tag{9}$$

where $\mathbb{I} \in \mathbb{R}^{N\times N}$ is the identity matrix and $(\cdot,\cdot)$ the standard $\mathbb{R}^N$-scalar product. By defining

$$C(U,\Lambda) := \Lambda - \min(0, \Lambda + (\boldsymbol{U} - \boldsymbol{\chi})), \tag{10}$$

the complementarity conditions in (9) reduce to $C(U,\Lambda) = 0$. Indeed, from the definition (10) , notice that if $\Lambda + (\boldsymbol{U} - \boldsymbol{\chi}) < 0 \implies C(U,\Lambda) = (\boldsymbol{\chi} - \boldsymbol{U})$ and so, $C(U,\Lambda) = 0$ implies $\boldsymbol{U} = \boldsymbol{\chi}$, which together with $\Lambda + (\boldsymbol{U} - \boldsymbol{\chi}) < 0$ gives $\Lambda < 0$. Similarly, $\Lambda + (\boldsymbol{U} - \boldsymbol{\chi}) > 0$ would imply $C(U,\Lambda) = \Lambda$. In this case the complementarity condition $C(U,\Lambda) = 0$ gives $\Lambda = 0$ which together with $\Lambda + (\boldsymbol{U} - \boldsymbol{\chi}) > 0$ yields $\boldsymbol{U} > \boldsymbol{\chi}$. Hence, the solution of (9) is reduced to solve the system

$$\mathbb{A}\,\boldsymbol{U} + \mathbb{I}\,\Lambda = \boldsymbol{F}, \qquad C(U,\Lambda) = 0. \tag{11}$$

The primal-dual active set algorithm solves (11) iteratively:
(i) Set $k = 0$, Initialise $\boldsymbol{U}^{(0)},\ \Lambda^{(0)}$.
(ii) Find the sets of vertices $\mathbb{AC}^{(k)}$ and $\mathbb{D}^{(k)}$ defined as

$$\mathbb{AC}^{(k)} = \{1 \le j \le N : \Lambda_j^{(k)} + (U_j^{(k)} - \boldsymbol{\chi}_j^{(k)}) < 0\} \quad \text{indices in active set,}$$
$$\mathbb{D}^{(k)} = \{1 \le j \le N : \Lambda_j^{(k)} + (U_j^{(k)} - \boldsymbol{\chi}_j^{(k)}) \ge 0\} \quad \text{indices not in active set.}$$

(iii) Solve for $(\boldsymbol{U}^{(k+1)}, \Lambda^{(k+1)})$ from the following system:

$$\mathbb{A}\,\boldsymbol{U}^{(k+1)} + \mathbb{I}\,\Lambda^{(k+1)} = \boldsymbol{F}, \quad U_j^{(k+1)} = \chi_j \ \ \forall j \in \mathbb{AC}^{(k)}, \qquad \Lambda_j^{(k+1)} = 0 \ \ \forall\, j \in \mathbb{D}^{(k)}.$$

(iv) Set $k = k + 1$. Go to Step (ii) and compute $\mathbb{AC}^{(k)}$ and its complementary $\mathbb{D}^{(k)}$. The iteration is stopped when $\mathbb{AC}^{(k)} = \mathbb{AC}^{(k+1)}$. The set $\mathbb{AC}^{(k)}$ contains the indices for the vertices in the discrete contact set $\mathbb{C}_h$; $\mathbb{D}^{(k)}$ contains the indices of the remaining nodes.

5.1 Numerical experiments

We present now some test examples to illustrate the performance of a-posteriori error estimator. For the adaptive refinement, we use the paradigm

$$\textbf{SOLVE} \longrightarrow \textbf{ESTIMATE} \longrightarrow \textbf{MARK} \longrightarrow \textbf{REFINE}$$

In the step SOLVE, we compute u_h using the primal-dual active set algorithm as described before. Thereafter, we compute the error estimator η_h on each element $T \in \mathcal{T}_h$ and use maximum marking strategy with parameter $\theta = 0.4$. Finally, the mesh is refined using the newest vertex bisection algorithm. In all examples, we set $\alpha_e = 25$ and $\mathbb{AC}$ refers to the discrete active set (depicted in yellow).

Example 1: Madonna's obstacle: (scaled version of [7, example 3.1])). Let $\Omega = (0,1)^2$, $f = 0$ and $r^2 = (x - 1/2)^2 + (y - 1/2)^2$, $\quad x, y \in \Omega$

$$\chi = 1 - 4r, \qquad u = \begin{cases} 1 - 4r, & r < 1/4 \\ -(\log(r) + 2\log(2)), & r \geq 1/4. \end{cases}$$

In Figure 1a we report the error and the estimator η_h. This graphic indicates a rate $(1/DOF)$ with respect to degrees of freedom (DOF). The single estimators η_i, $i = 1...6$ are plotted in Figure 1b. Both graphics confirm the reliability of the estimator. In Figure 2 are depicted the efficiency indices (leftmost subfigure), the adaptive mesh refinement at level 20 (center) and the discrete contact set $\mathbb{C}_h$ (rightmost figure). Note that the solution is singular in the $\mathbb{C}$ due to the singularity of the obstacle therein, which leads to the more refinement in $\mathbb{C}_h$. Also as expected, we observe more refinement near free boundary.

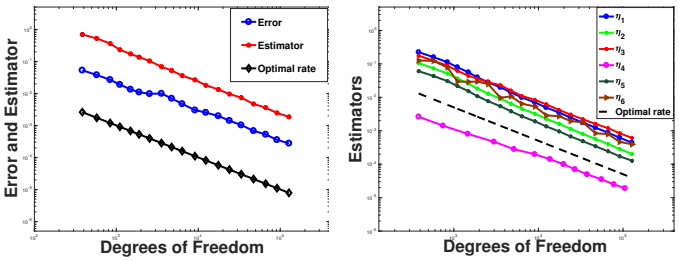

(a) Error and Estimator

(b) Estimator contributions

Fig. 1: Example 1: Error, Estimator and estimator contributions

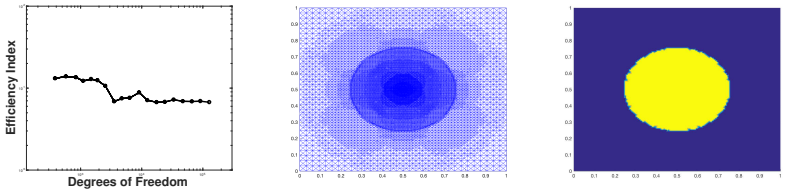

Fig. 2: Example 1: Efficiency index, adaptive mesh and $\mathbb{AC}$

Example 2: non-convex domain [2]:

$$\Omega = (-2, 2)^2 \setminus [0, 2) \times (-2, 0], \qquad \chi = 0,$$

$$u = r^{2/3} sin(2\theta/3)\gamma_1(r), \qquad r^2 = x^2 + y^2\,, \qquad \tilde{r} = 2(r - 1/4)$$

$$f = -r^{2/3} sin(2\theta/3)\left(\frac{\gamma_1'(r)}{r} + \gamma_1''(r)\right) - \frac{4}{3} r^{-1/3} sin(2\theta/3)\gamma_1'(r) - \gamma_2(r)$$

$$\gamma_1(r) = \begin{cases} 1, & \tilde{r} < 0 \\ -6\tilde{r}^5 + 15\tilde{r}^4 - 10\tilde{r}^3 + 1, & 0 \le \tilde{r} < 1 \\ 0, & \tilde{r} \ge 1, \end{cases} \qquad \gamma_2(r) = \begin{cases} 0, & r \le \frac{5}{4} \\ 1, & \text{otherwise.} \end{cases}$$

In Figure 3(a) we compare the estimator η_h with the one in energy norm. From this graphic, it is evident that the error and the estimator converge with rate $1/DOF$ in L^∞ and $1/\sqrt{DOF}$ in energy norm. The convergence behaviour of the single estimators η_i, $i = 1...6$ is given in Figure 3(b). Note that, η_5 is zero since $\chi = \chi_h = 0$ in this example. Figure 4 confirms the efficiency of the estimator η_h. In Figure 4 are also given the adaptive mesh refinement at the level 24 and $\mathbb{C}_h$. We observe that the estimator captures well the singular behavior of the solution. The mesh refinement near the free boundary is higher due to the large jump in gradients.

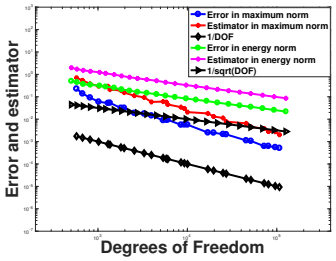

(a) Error and Estimator

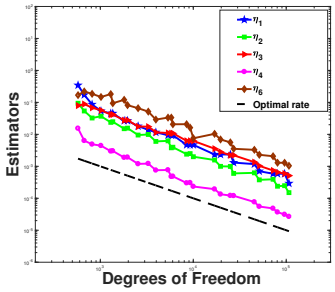

(b) Estimators in maximum norm

Fig. 3: Example 2: Error and estimator in energy norm and maximum norm and single estimators in maximum norm.

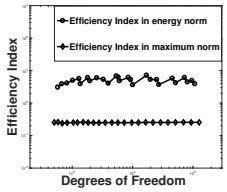

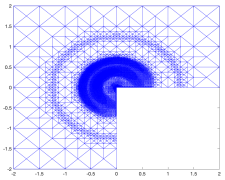

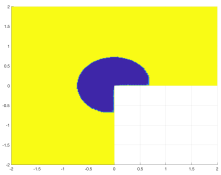

Fig. 4: Example 2: Efficiency index in energy norm and maximum norm, adaptive mesh and $\mathbb{AC}$

Example 3: taken from [6] (Liptschiz obstacle):

$$\Omega = \{(x, y) \in \mathbb{R}^2 : |x| + |y| < 1\}, \quad f = -5, \qquad \chi = \text{dist}(x, \partial\Omega) - 1/5.$$

In Figure 5 we have reported the estimator η_h and the single estimators η_i, $i = 1...6$, ($\eta_5 = 0$ since χ is piecewise linear) (leftmost) together with the adaptive mesh at refinement level 7 (center) and $\mathbb{C}_h$ (rightmost). It can be observed that the estimator converges with the optimal rate. The obstacle function is in the shape of a pyramid

and the continuous Lagrange multiplier has support along the edges of the obstacle which justifies the refinement along the edges of the obstacle in the contact region.

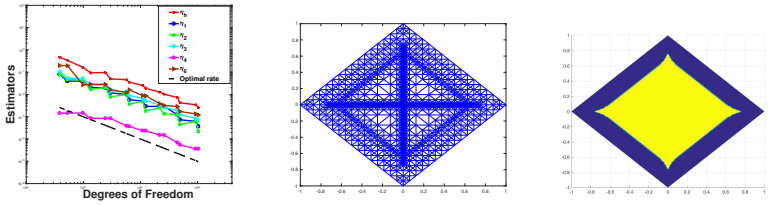

Fig. 5: Example 3: Estimators, Adaptive Mesh and $\mathbb{AC}$

References

1. B. Ayuso de Dios, T. Gudi, and K. Porwal. Pointwise a posteriori error analysis of a discontinuous Galerkin method for the elliptic obstacle problem. *arXiv:2108.11611 [math.NA]*.
2. D. Braess, C. Carstensen, and R. H. W. Hoppe. Convergence analysis of a conforming adaptive finite element method for an obstacle problem. *Numer. Math.*, 107:455–471, 2007.
3. R. Glowinski. *Numerical Methods for Nonlinear Variational Problems*. Springer-Verlag, Berlin, 2008.
4. T. Gudi and K. Porwal. A posteriori error control of discontinuous Galerkin methods for elliptic obstacle problems. *Math. Comp.*, 83:579–602, 2014.
5. M. Hintermüller, K. Ito, and K. Kunish. The primal-dual active set strategy as a semismooth Newton method. *SIAM J. Optim.*, 13:865–888, 2003.
6. R.H. Nochetto, K. G. Siebert, and A. Veeser. Pointwise a posteriori error control for elliptic obstacle problems. *Numer. Math.*, 95:163–195, 2003.
7. R.H. Nochetto, K. G. Siebert, and A. Veeser. Fully localized a posteriori error estimators and barrier sets for contact problems. *SIAM J. Numer. Anal.*, 42(5):2118–2135, 2005.
8. A. Veeser. Efficient and reliable a posteriori error estimators for elliptic obstacle problems. *SIAM J. Numer. Anal.*, 39:146–167, 2001.